Passively Mode-Locked Raman Laser

W. Liang, V. S. Ilchenko, A. A. Savchenkov, A. B. Matsko, D. Seidel, and L. Maleki
OEwaves Inc., 2555 E. Colorado Blvd., Ste. 400, Pasadena, California 91107, USA
(Received 10 May 2010; revised manuscript received 20 July 2010; published 30 September 2010)

We report on the observation of a mode-locked laser generated with a crystalline whispering gallery mode resonator pumped with a continuous wave laser. Optical pumping of the resonator generates an optical frequency comb with phase locked components at the Raman offset of the resonator host material. Phase locking of the modes is confirmed via measurement of the radio-frequency beat note produced by the comb on a fast photodiode. Neither the conventional Kerr comb nor hyperparametric oscillation is observed when the comb is present. We present a theoretical explanation of the effect.

DOI: 10.1103/PhysRevLett.105.143903 PACS numbers: 42.55.Ye, 42.55.Sa, 42.60.Fc, 42.65.Ky

Ultralow threshold stimulated Raman scattering (SRS) and four-wave mixing (FWM) [1] are among numerous nonlinear phenomena observed in whispering gallery mode (WGM) resonators. FWM results in hyperparametric oscillations and generation of optical frequency (Kerr) combs possessing excellent uniformity of spectral lines [2–13]. In this Letter we report on the discovery of a novel phase locked optical frequency comb generated at the Raman frequency offset of the WGM resonator host material (Raman comb). We argue that the comb is different from the Kerr comb, as well as from multimode SRS previously observed in WGM resonators, and is the spectral signature of a novel passively mode-locked laser. We theoretically show that these Raman combs are produced in a novel regime of mode locking that requires the presence of both the Raman gain and the FWM process.

SRS was studied since the early days of WGM resonators, first in liquid droplets [14,15] and then in high-Q fused silica microresonators [1]. It was shown that the resonant Raman process starts with low pump powers, at the microwatt level, and that the efficiency of frequency conversion in the Raman laser is very high [16,17]. The possibility of generation of numerous higher order Stokes lines was also demonstrated [17,18].

The resonant FWM has nearly the same efficiency as SRS, so that hyperparametric oscillation and Raman lasing compete in WGM resonators [15,19]. SRS tends to have lower threshold in larger resonators. This is because, in contrast to FWM, the lasing process does not require phase matching, and Stokes light is generated in an arbitrary mode having a higher quality factor and better overlap with the pumping mode. Stokes lines may involve several WGMs. Light generated in each mode represents an independent laser, so there is no phase dependence among the modes. If SRS starts at a lower pump power, the harmonics of the Stokes component fold down to the frequency of the pump, forming optical sidebands resembling those produced by hyperparametric oscillation. Since the Stokes signal and the pump are mutually independent, down-converted sidebands and the pump have low mutual coherence. In this way, the SRS process diminishes the quality of the optical Kerr comb produced with low enough pump power [20]. Higher pump power can result in the overlap of Kerr and Raman combs, and in the generation of a joint mode-locked comb [2]. In some regimes, though, SRS results in an appreciable nonlinear loss for the pump radiation, and drains the pump so fast that no Kerr comb is formed at any pump power [17].

We have discovered that Stokes SRS harmonics generated in a CaF_2 WGM resonator can be phase locked, and actually be mutually coherent. In other words, the harmonics form a coherent Raman comb. The phase locking occurs for specific values of dispersion, nonlinearity, and the width of the Raman gain. In such a regime, no high order Stokes modes [17,18] are generated, and no hyperparametric oscillation is observed. To confirm that mode locking does occur, we have measured the spectral purity and instantaneous linewidth of the rf signal generated by the beat of the Raman comb on a fast photodiode. We have directly observed the collapsing of the linewidth of the rf signal when the mode locking regime was achieved. The low phase noise of the rf signal is indicative of the high efficacy of mode locking in the Raman comb.

We explain these observations using the notion of passive mode locking developed several decades ago [21–23]. Mode locking occurs by the proper interplay between dispersion and nonlinearity in materials that possess optical (Raman, in our case) gain. The mode locking phenomenon reported here is different from the effect studied in lumped systems, since gain, nonlinearity, and dispersion are truly distributed in our case. The physics behind the observed phenomenon is also different from the physics of Kerr combs, as the phase of the generated light is independent of the phase of the pumping light in this mode-locked Raman laser. Moreover, the detuning of the pump frequency from the corresponding WGM eigenfrequency ensures that the phase matching condition necessary for hyperparametric oscillation occurs [19], while the Raman modes are, to a first approximation, generated at frequencies independent from the pump laser frequency.

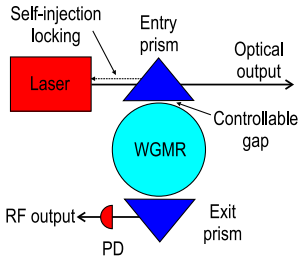

FIG. 1 (color online). Schematic of the experimental setup. Light from the pump laser enters the whispering gallery mode resonator (WGMR) through the input prism. The light exiting the input prism is collimated and sent to an optical spectrum analyzer. The output light from the output prism is sent to a fast photodiode (PD).

Our observations pave the road for the development of a new class of mode-locked lasers based on continuous wave pumped WGM resonators. The fundamental advantage of these lasers draws from the extremely high Q factors of modes of the active optical resonator that ensure high quality mode locking with small input power, and the high stability of lasing is independent of the quality of the laser used for pumping. A practical advantage of mode-locked Raman lasers is their small size and low power consumption.

To realize a WGM mode-locked Raman laser one needs a pumping laser, a WGM resonator made out of a transparent material possessing cubic nonlinearity, an evanescent field coupling element, and supportive optics. We used a distributed-feedback (DFB) laser, a CaF_2 resonator, and two glass prism couplers (Fig. 1). The pump laser produced 6 mW of power at 1532 nm, and we were able to couple about 2 mW into the WGM resonator. The resonator had 1.9 mm diameter and 0.1 mm thickness. The rim of the resonator was shaped to maximize optical coupling [24]. The unloaded Q factor of the resonator was larger than 10^9, and loading with the prisms reduced the Q to 5×10^8. We were able to monitor and change the degree of loading of the WGM by changing the distance between the coupling prisms and the resonator surface. The laser was self-injection locked to a selected WGM. Injection locking reduced the 2 MHz linewidth of the free running DFB laser to less than 200 Hz [24], which allowed us to pump the high-Q WGM efficiently.

With an optimal value of the optical power and optimal tuning of the pumping laser we achieved generation of the Raman frequency comb shown in Fig. 2. The shape of the envelope of this comb is similar to the shape of the Raman comb observed in silica microspheres [1]. There were no satellite sidebands generated around the carrier frequency of the pumping mode, as was the case with the silica resonator. By varying the pumping frequency with respect to the corresponding WGM it was possible to generate minor FWM-mediated sidebands; however, these sidebands had at least 30 dB lower power as compared with the power

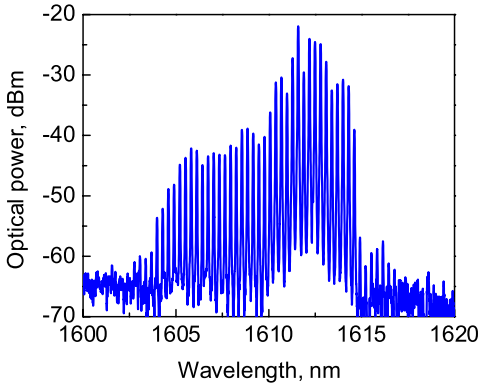

FIG. 2 (color online). Optical frequency comb formed at the first Stokes line of the CaF_2 WGM resonator. Neither the second Stokes line (expected at 1699 nm) nor the FWM sidebands around the carrier are observed. The comb has approximately 10 nm spectral width.

of the pump. Hence, it is safe to say that no hyperparametric oscillation took place. In addition, we did not observe the second order Stokes line, expected at 1699 nm. These facts indicate that the first order SRS process is very efficient. To confirm this, we estimated that the power of the Stokes light emitted in the forward direction through the entry prism was approximately -16 dBm (we only collected approximately 10% light escaping the input prism so the number is good for comparison only), so the total power emitted in the Raman modes through the input prism (both directions) is -13 dBm. To compare, the pump power exiting the resonator through the input prism was -18 dBm. Hence, the efficiency of the Raman laser exceeds 50%.

We studied the rf signal generated by the Raman comb with a fast photodiode and found that the signal frequency was 35 GHz and its instantaneous linewidth was less than 100 Hz. We measured the phase noise of the signal and found that it is quite low (Fig. 3). These observations confirm that the modes in the Raman comb are mutually coherent, and that this Raman laser operates in the

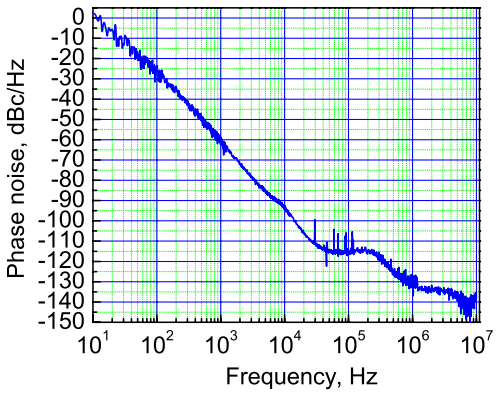

FIG. 3 (color online). Single sideband phase noise of the rf signal generated by the Raman comb (Fig. 2) on a fast photodiode.

mode-locked regime. This is the basic result of the reported experimental research.

To explain the formation of the phase locked Raman comb we use the theory developed for passive mode-locked lasers [21–23], and start from the master equation describing propagation of an optical pulse in a nonlinear, dispersive, and amplifying medium

$$T_a\frac{\partial A}{\partial T}+\frac{i}{2}\left(\beta_{2\Sigma}+\frac{i}{\Omega_f^2}\right)\frac{\partial^2 A}{\partial t^2} = i\gamma_\Sigma|A|^2A+\frac{1}{2}(g_\Sigma|A_p|^2-\alpha_\Sigma)A, \quad (1)$$

where $A(T, t)$ is the slowly varying envelope of the electric field, $T = z/V_g$, $T_a = 2\pi a/V_g$ is the round-trip time in the resonator, V_g is the group velocity, $\gamma_\Sigma = 2\pi a\gamma_2$ is the third-order nonlinearity summed up over the length of the optical path, $\gamma_2 = n_2\omega_0/c\mathcal{A}$, ω_0 is the optical frequency, $g_\Sigma = (2\pi a/\mathcal{A})G$ and $\alpha_\Sigma = T_a\Gamma$ are the integrated loop gain and attenuation, G is the bulk Raman gain of the material (in cm/W), $\mathcal{A}$ is the cross-sectional area of the mode, Γ is the full width at half maximum (FWHM) of the optical resonance (in rad/s), $\beta_{2\Sigma}$ is the integral second order dispersion, and $A_p(T)$ is the pump light amplitude.

To characterize the gain of the Raman laser we write the equation for the pump [25]

$$T_a\frac{\partial A_p}{\partial T}+\frac{1}{2}\left(g_\Sigma\frac{E}{T_a}+\alpha_\Sigma\right)A_p=\sqrt{\alpha_{c\Sigma}P}, \quad (2)$$

where $\alpha_{c\Sigma}$ is the attenuation caused by the coupling only, P is the value of the external pump power, and E is the pulse energy (for the case of the fundamental mode locking),

$$E=\int_{-T_a/2}^{T_a/2}|A(T, t)|^2dt. \quad (3)$$

We assume that (i) the bulk Raman gain G has a Lorentzian spectral shape (the parabolic filtering effect) with FWHM Δ_ω, so the effective spectral width of the gain is defined as $\Omega_f = \Delta_\omega/2|A_p|g_\Sigma^{1/2}$, (ii) the optical loop is operating in the mode-locked regime and that the optical field is not changed significantly during the round-trip time of the optical pulse (T_a), (iii) both the optical gain and the nonlinearity are fast compared with the duration of the optical pulse, and (iv) the pulse shape is given by

$$A(T, t)=\left[\frac{E}{\sqrt{\pi}\tau}\right]^{1/2}\left[\exp-\left(\frac{t-\xi}{\sqrt{2}\tau}\right)^2\right]^{1+iq}e^{i\Omega(t-\xi)}, \quad (4)$$

where ξ is the temporal shift (timing), Ω is the frequency shift, q is the chirp, and τ is the pulse duration.

We derive the steady state equations for the five parameters describing the optical pulses (4) using the standard technique [26–28]. We define slow amplitudes as

$$E(T)=\int_{-\infty}^{\infty}|A(T, t)|^2dt, \quad (5)$$

$$\xi(T)=\frac{1}{E}\int_{-\infty}^{\infty}t|A(T, t)|^2dt, \quad (6)$$

$$\Omega(T)=-\frac{i}{2E}\int_{-\infty}^{\infty}\left[A^*\frac{\partial A}{\partial t}-A\frac{\partial A^*}{\partial t}\right]dt, \quad (7)$$

$$q(T)=\frac{i}{E}\int_{-\infty}^{\infty}(t-\xi)\left[A^*\frac{\partial A}{\partial t}-A\frac{\partial A^*}{\partial t}\right]dt, \quad (8)$$

$$\tau^2(T)=\frac{2}{E}\int_{-\infty}^{\infty}(t-\xi)^2|A(T, t)|^2dt. \quad (9)$$

The time independent propagation equations for the parameters can be found by direct differentiation of Eqs. (5)–(9)

$$\frac{dE}{dT}=\int_{-\infty}^{\infty}\left[A^*\frac{\partial A}{\partial T}+A\frac{\partial A^*}{\partial T}\right]dt, \quad (10)$$

$$\frac{d\xi}{dT}=\frac{1}{E}\int_{-\infty}^{\infty}(t-\xi)\left[A^*\frac{\partial A}{\partial T}+A\frac{\partial A^*}{\partial T}\right]dt, \quad (11)$$

$$\frac{d\Omega}{dT}=-\frac{1}{E}\frac{dE}{dT}\Omega-\frac{i}{2E}\int_{-\infty}^{\infty}\left[\frac{\partial}{\partial T}\left(A^*\frac{\partial A}{\partial t}\right)-\frac{\partial}{\partial T}\left(A\frac{\partial A^*}{\partial t}\right)\right]dt, \quad (12)$$

$$\frac{dq}{dT}=-\frac{1}{E}\frac{dE}{dT}q+\frac{i}{E}\int_{-\infty}^{\infty}(t-\xi)\left[\frac{\partial}{\partial T}\left(A^*\frac{\partial A}{\partial t}\right)-\frac{\partial}{\partial T}\left(A\frac{\partial A^*}{\partial t}\right)\right]dt, \quad (13)$$

$$\tau\frac{d\tau}{dT}=-\frac{1}{2E}\frac{dE}{dT}\tau^2+\frac{1}{E}\int_{-\infty}^{\infty}(t-\xi)^2\left[A^*\frac{\partial A}{\partial T}+A\frac{\partial A^*}{\partial T}\right]dt. \quad (14)$$

For the sake of simplicity we assume that $\xi = 0$, $\Omega = 0$, and a set of three equations remains

$$g_\Sigma|A_p|^2-\alpha_\Sigma-\frac{1+q^2}{2\tau^2\Omega_f^2}=0, \quad (15)$$

$$\left[\frac{\beta_{2\Sigma}}{\tau^2}-\frac{q}{\tau^2\Omega_f^2}\right](1+q^2)+\frac{E\gamma_\Sigma}{\sqrt{2\pi}\tau}=0, \quad (16)$$

$$q\frac{\beta_{2\Sigma}}{\tau}+\frac{1-q^2}{2\tau\Omega_f^2}=0. \quad (17)$$

The energy of the pulse can be found from Eqs. (2) and (15). We assume that the last term in Eq. (15) is small and derive

$$|A_p|^2=\frac{\alpha_\Sigma}{g_\Sigma}, \quad (18)$$

$$E=\left(2\sqrt{g_\Sigma P\frac{\alpha_{c\Sigma}}{\alpha_\Sigma}}-\alpha_\Sigma\right)\frac{T_a}{g_\Sigma}. \quad (19)$$

According to Eq. (19) the threshold pump power is given by

$$P_{\text{th}}=\frac{\alpha_\Sigma^2}{4g_\Sigma}\frac{\alpha_\Sigma}{\alpha_{c\Sigma}}. \quad (20)$$

We also find from Eqs. (16) and (17)

$$\tau = \frac{2\sqrt{2\pi}}{E\gamma_\Sigma \Omega_f^2}(\beta_{2\Sigma}^2\Omega_f^4 + 1)(\beta_{2\Sigma}\Omega_f^2 + \sqrt{\beta_{2\Sigma}^2\Omega_f^4 + 1}), \tag{21}$$

$$q = \beta_{2\Sigma}\Omega_f^2 + \sqrt{\beta_{2\Sigma}^2\Omega_f^4 + 1}. \tag{22}$$

The calculations show that the model has a viable physical solution which means that the Raman laser generates optical pulses, and explains, in principle, the experimental observation.

Let us estimate the parameters of pulses generated in our laser. To do this we first should evaluate the numerical values of parameters used in Eq. (1). Calculating the resultant dispersion of the resonator using Sellmeiers dispersion equation [29] for bulk material, together with the expression for geometrical dispersion of the basic sequence of WGMs [30] we found that combs tend to appear at small *normal* group velocity dispersion $\beta_2 = 3\ \mathrm{ps}^2/\mathrm{km}$, so that $\beta_{2\Sigma} = 1.8 \times 10^{-29}\ \mathrm{s}^2$. The Kerr nonlinearity coefficient is given by $n_2 = 3 \times 10^{-16}\ \mathrm{cm}^2/\mathrm{W}$ and $\mathcal{A} \simeq 10^{-6}\ \mathrm{cm}^2$, so that $\gamma_2 = 1.3 \times 10^{-5}\ \mathrm{cm}^{-1}\,\mathrm{W}^{-1}$ and $\gamma_\Sigma = 7.5 \times 10^{-6}\ \mathrm{W}^{-1}$. The bulk Raman gain is $G = 1.5 \times 10^{-11}\ \mathrm{cm/W}$, so that $g_\Sigma = 9 \times 10^{-6}\ \mathrm{W}^{-1}$. The spectral width of the Raman gain is $\Delta_\omega = 2\pi \times 4.5 \times 10^{11}\ \mathrm{s}^{-1}$, $\alpha_\Sigma = 7.2 \times 10^{-5}$. Assuming that $g_\Sigma|A_p|^2 \approx \alpha_\Sigma$, we find $\Omega_f \simeq 1.7 \times 10^{14}\ \mathrm{s}^{-1}$. Finally, we assume that $\alpha_{c\Sigma} = \alpha_\Sigma/2$ and $P = 2$ mW. Taking these values into account, we find $q = 1.6$, $E = 40$ nJ, and $\tau = 0.1$ ps. The threshold power is $P_{\mathrm{th}} = 0.3$ mW. Therefore, theoretically, the laser generates subpicosecond pulses. An additional study is required to prove the stability of this solution and to observe any pulses.

To conclude, we have experimentally demonstrated and theoretically explained a mode-locked Raman comb in a CaF_2 WGM resonator. The comb manifests itself when the frequency of the Stokes Raman line approaches, but does not overlap with, the zero-group velocity frequency region of the WGM spectrum. Upon demodulation on a fast photodiode, the comb generates a spectrally pure rf signal at a frequency corresponding to the repetition rate of the optical comb. This comb is different from the Kerr comb and from passively mode-locked lasers, and clearly represents another physical phenomenon uniquely observable in high-Q WGM resonators.

The authors acknowledge Danny Eliyahu's help with the phase noise measurement of the rf signal.

[1] S. M. Spillane, T. J. Kippenberg, and K. J. Vahala, Nature (London) **415**, 621 (2002).
[2] P. Del'Haye *et al.*, Nature (London) **450**, 1214 (2007).
[3] P. Del'Haye *et al.*, Phys. Rev. Lett. **101**, 053903 (2008).
[4] A. A. Savchenkov *et al.*, Phys. Rev. Lett. **101**, 093902 (2008).
[5] I. S. Grudinin, N. Yu, and L. Maleki, Opt. Lett. **34**, 878 (2009).
[6] I. H. Agha, Y. Okawachi, and A. L. Gaeta, Opt. Express **17**, 16 209 (2009).
[7] J. S. Levy *et al.*, Nat. Photon. **4**, 37 (2010).
[8] L. Razzari *et al.*, Nat. Photon. **4**, 41 (2010).
[9] D. Braje, L. Hollberg, and S. Diddams, Phys. Rev. Lett. **102**, 193902 (2009).
[10] P. Del'Haye *et al.*, arXiv:0912.4890v1.
[11] O. Arcizet *et al.*, in *Practical Applications of Microresonators in Optics and Photonics*, edited by A. B. Matsko (CRC Press, Boca Raton, Florida, 2009), Chap. 11.
[12] A. B. Matsko *et al.*, in *Proc. of 7th Symp. Frequency Standards and Metrology*, edited by L. Maeki (World Scientific, New Jersey, 2009), p. 539.
[13] Y. K. Chembo, D. V. Strekalov, and N. Yu, Phys. Rev. Lett. **104**, 103902 (2010).
[14] S.-X. Qian, J. B. Snow, and R. K. Chang, Opt. Lett. **10**, 499 (1985).
[15] H.-B. Lin and A. J. Campillo, Phys. Rev. Lett. **73**, 2440 (1994).
[16] T. J. Kippenberg *et al.*, IEEE J. Sel. Top. Quantum Electron. **10**, 1219 (2004).
[17] I. S. Grudinin and L. Maleki, Opt. Lett. **32**, 166 (2007).
[18] B. Min, T. J. Kippenberg, and K. J. Vahala, Opt. Lett. **28**, 1507 (2003).
[19] A. B. Matsko *et al.*, Phys. Rev. A **71**, 033804 (2005).
[20] A. A. Savchenkov *et al.*, Opt. Express **16**, 4130 (2008).
[21] O. E. Martinez, R. L. Fork, and J. P. Gordon, Opt. Lett. **9**, 156 (1984).
[22] H. A. Haus and Y. Silberberg, IEEE J. Quantum Electron. **22**, 325 (1986).
[23] H. A. Haus, IEEE J. Sel. Top. Quantum Electron. **6**, 1173 (2000).
[24] L. Maleki *et al.*, in *Practical Applications of Microresonators in Optics and Photonics*, edited by A. B. Matsko (CRC Press, Boca Raton, Florida, 2009), Chap. 3.
[25] A. B. Matsko, A. A. Savchenkov, and L. Maleki, Opt. Commun. **260**, 662 (2006).
[26] N. Usechak and G. Agrawal, Opt. Express **13**, 2075 (2005).
[27] F. Rana, R. J. Ram, and H. A. Haus, IEEE J. Quantum Electron. **40**, 41 (2004).
[28] H. A. Haus and A. Mecozzi, IEEE J. Quantum Electron. **29**, 983 (1993).
[29] M. Daimon and A. Masumura, Appl. Opt. **41**, 5275 (2002).
[30] A. B. Matsko *et al.*, J. Opt. Soc. Am. B **20**, 2292 (2003).